

MOA-2010-BLG-523: “Failed Planet” = RS CVn Star¹

A. Gould¹, J.C. Yee¹, I.A. Bond², A. Udalski³, C. Han⁴, U.G. Jørgensen^{5,6}, J. Greenhill⁷,
Y. Tsapras^{8,9}, M.H. Pinsonneault¹, T. Bensby¹⁰

and

W. Allen¹¹, L.A. Almeida¹², M. Bos¹³, G.W. Christie¹⁴, D.L. DePoy¹⁵, Subo Dong^{16,1},
B.S. Gaudi¹, L.-W. Hung¹, F. Jablonski¹², C.-U. Lee¹⁷, J. McCormick¹⁸, D. Moorhouse¹⁹,
J.A. Muñoz²⁰, T. Natusch^{14,21}, M. Nola¹⁹, R.W. Pogge¹, J. Skowron¹, G. Thornley¹⁹

(The μ FUN Collaboration),

F. Abe²², D.P. Bennett^{23,24}, C.S. Botzler²⁵, P. Chote²⁶, M. Freeman²⁵, A. Fukui²⁷,
K. Furusawa²², P. Harris²⁶, Y. Itow²², C.H. Ling², K. Masuda²², Y. Matsubara²²,
N. Miyake²², K. Ohnishi²⁸, N.J. Rattenbury²⁵, To. Saito²⁹, D.J. Sullivan²⁶, T. Sumi^{30,22},
D. Suzuki³⁰, W.L. Sweatman², P.J. Tristram³¹, K. Wada³⁰, P.C.M. Yock²⁵

(The MOA Collaboration),

M.K. Szymański³, I. Soszyński³, M. Kubiak³, R. Poleski³, K. Ulaczyk³, G. Pietrzyński^{3,32},
Ł. Wyrzykowski^{3,33}

(The OGLE Collaboration),

K.A. Alsubai³⁴, V. Bozza^{35,36}, P. Browne^{37,38}, M.J. Burgdorf^{39,40}, S. Calchi Novati^{35,41},
P. Dodds³⁷, M. Dominik^{37,42,38}, F. Finet⁴³, T. Gerner⁴⁴, S. Hardis⁵, K. Harpsøe^{5,6},
F.V. Hessman⁴⁵, T.C. Hinse^{5,46,17}, M. Hundertmark^{37,45}, N. Kains^{47,37,38}, E. Kerins⁴⁸,
C. Liebig^{37,44}, L. Mancini^{35,49}, M. Mathiasen⁵, M.T. Penny^{1,48}, S. Proft⁴⁴, S. Rahvar^{50,51},
D. Ricci⁴³, K.C. Sahu⁵², G. Scarpetta^{35,36}, S. Schäfer⁴⁵, F. Schönebeck⁴⁴,
C. Snodgrass^{53,54,38}, J. Southworth⁵⁵, J. Surdej⁴⁵, J. Wambsganss⁴⁴

(The MiNDSTEp Consortium)

R.A. Street⁸, K. Horne³⁷, D.M. Bramich⁴⁷, I.A. Steele⁵⁶

(The RoboNet Collaboration),

M.D. Albrow⁵⁷, E. Bachelet⁵⁸, V. Batista^{1,59}, T.G. Beatty¹, J.-P. Beaulieu⁵⁹,
C.S. Bennett⁶⁰, R. Bowens-Rubin⁶¹, S. Brilliant⁶², J.A.R. Caldwell⁶³, A. Cassan⁵⁹,
A.A. Cole⁷, E. Corrales⁵⁹, C. Coutures⁵⁹, S. Dieters⁷, D. Dominis Prester⁶⁴,
J. Donatowicz⁶⁵, P. Fouqué⁵⁸, C.B. Henderson¹, D. Kubas^{62,59}, J.-B. Marquette⁵⁹,
R. Martin⁶⁶, J.W. Menzies⁶⁷, B. Shappee¹, A. Williams⁶⁶, J. van Saders¹, M. Zub⁴⁴,

(The PLANET Collaboration)

¹Department of Astronomy, Ohio State University, 140 West 18th Avenue, Columbus, OH 43210, USA

²Institute for Information and Mathematical Sciences, Massey University, Private Bag 102-904, Auckland 1330, New Zealand

³Warsaw University Observatory, Al. Ujazdowskie 4, 00-478 Warszawa, Poland

⁴Department of Physics, Chungbuk National University, Cheongju 361-763, Korea

⁵Niels Bohr Institutet, Københavns Universitet, Juliane Maries Vej 30, 2100 Copenhagen, Denmark

⁶Centre for Star and Planet Formation, Geological Museum, Øster Voldgade 5, 1350 Copenhagen, Denmark

⁷University of Tasmania, School of Mathematics and Physics, Private Bag 37, Hobart, TAS 7001, Australia

⁸Las Cumbres Observatory Global Telescope Network, 6740B Cortona Dr, Goleta, CA 93117, USA

⁹School of Physics and Astronomy, Queen Mary University of London, Mile End Road, London, E1 4NS

¹⁰Lund Observatory, Department of Astronomy and Theoretical physics, Box 43, SE-221 00 Lund, Sweden

¹¹Vintage Lane Observatory, Blenheim, New Zealand

¹²Divisao de Astrofisica, Instituto Nacional de Pesquisas Espaciais, Avenida dos Astronautas, 1758 Sao José dos Campos, 12227-010 SP, Brasil

¹³Molehill Astronomical Observatory, North Shore, New Zealand

¹⁴Auckland Observatory, Auckland, New Zealand

¹⁵Department of Physics and Astronomy, Texas A&M University, College Station, Texas 77843-4242, USA

¹⁶Institute for Advanced Study, Einstein Drive, Princeton, NJ 08540, USA

¹⁷Korea Astronomy and Space Science Institute, 776 Daedukdae-ro, Yuseong-gu, Daejeon 305-348, Republic of Korea

¹⁸Farm Cove Observatory, Centre for Backyard Astrophysics, Pakuranga, Auckland, New Zealand

¹⁹Kumeu Observatory, Kumeu, New Zealand

²⁰Departamento de Astronomía y Astrofísica, Universidad de Valencia, E-46100 Burjassot, Valencia, Spain

²¹AUT University, Auckland, New Zealand

²²Solar-Terrestrial Environment Laboratory, Nagoya University, Nagoya, 464-8601, Japan

²³Department of Physics, 225 Nieuwland Science Hall, University of Notre Dame, Notre Dame, IN 46556, USA

²⁴Also PLANET Collaboration

²⁵Department of Physics, University of Auckland, Private Bag 92-019, Auckland 1001, New Zealand

²⁶School of Chemical and Physical Sciences, Victoria University, Wellington, New Zealand

²⁷Okayama Astrophysical Observatory, National Astronomical Observatory, 3037-5 Honjo, Kamogata,

Asakuchi, Okayama 719-0232, Japan

²⁸Nagano National College of Technology, Nagano 381-8550, Japan

²⁹Tokyo Metropolitan College of Aeronautics, Tokyo 116-8523, Japan

³⁰Department of Earth and Space Science, Graduate School of Science, Osaka University, 1-1 Machikaneyama-cho, Toyonaka, Osaka 560-0043, Japan

³¹Mt. John University Observatory, P.O. Box 56, Lake Tekapo 8770, New Zealand

³²Universidad de Concepción, Departamento de Astronomía, Casilla 160–C, Concepción, Chile

³³Institute of Astronomy, University of Cambridge, Madingley Road, Cambridge CB3 0HA, UK

³⁴Qatar Foundation, P.O. Box 5825, Doha, Qatar

³⁵Dipartimento di Fisica "E.R. Caianiello", Università degli Studi di Salerno, Via Ponte Don Melillo, 84084 Fisciano, Italy

³⁶INFN, Sezione di Napoli, Italy

³⁷SUPA, University of St Andrews, School of Physics & Astronomy, North Haugh, St Andrews, KY16 9SS, UK

³⁸Also RoboNet Collaboration

³⁹Deutsches SOFIA Institut but, HE Space Operations, Flughafenallee 26, 28199 Bremen, Germany

⁴⁰SOFIA Science Center, NASA Ames Research Center, Mail Stop N211-3, Moffett Field CA 94035, USA

⁴¹Istituto Internazionale per gli Alti Studi Scientifici (IIASS), Vietri Sul Mare (SA), Italy

⁴²Royal Society University Research Fellow

⁴³Institut d'Astrophysique et de Géophysique, Allée du 6 Août 17, Sart Tilman, Bât. B5c, 4000 Liège, Belgium

⁴⁴Astronomisches Rechen-Institut, Zentrum für Astronomie der Universität Heidelberg (ZAH), Mönchhofstr. 12-14, 69120 Heidelberg, Germany

⁴⁵Institut für Astrophysik, Georg-August-Universität, Friedrich-Hund-Platz 1, 3707,7 Göttingen, Germany

⁴⁶Armagh Observatory, College Hill, Armagh, BT61 9DG, Northern Ireland, UK

⁴⁷ESO Headquarters, Karl-Schwarzschild-Str. 2, 85748 Garching bei München, Germany

⁴⁸Jodrell Bank Centre for Astrophysics, University of Manchester, Oxford Road, Manchester, M13 9PL, UK

⁴⁹Max Planck Institute for Astronomy, Königstuhl 17, 69117 Heidelberg, Germany

⁵⁰Department of Physics, Sharif University of Technology, P. O. Box 11155–9161, Tehran, Iran

⁵¹Perimeter Institute for Theoretical Physics, 31 Caroline St. N., Waterloo ON, N2L 2Y5, Canada

⁵²Space Telescope Science Institute, 3700 San Martin Drive, Baltimore, MD 21218, USA

ABSTRACT

The Galactic bulge source MOA-2010-BLG-523S exhibited short-term deviations from a standard microlensing lightcurve near the peak of an $A_{\text{max}} \sim 265$ high-magnification microlensing event. The deviations originally seemed consistent with expectations for a planetary companion to the principal lens. We combine long-term photometric monitoring with a previously published high-resolution spectrum taken near peak to demonstrate that this is an RS CVn variable, so that planetary microlensing is not required to explain the lightcurve deviations. This is the first spectroscopically confirmed RS CVn star discovered in the Galactic bulge.

Subject headings: stars:spots – stars:variables:other – gravitational lensing – planetary systems

⁵³European Southern Observatory (ESO)

⁵⁴Max Planck Institute for Solar System Research, Max-Planck-Str. 2, 37191 Katlenburg-Lindau, Germany

⁵⁵Astrophysics Group, Keele University, Staffordshire, ST5 5BG, UK

⁵⁶Astrophysics Research Institute, Liverpool John Moores University, Liverpool CH41 1LD, UK

⁵⁷University of Canterbury, Department of Physics and Astronomy, Private Bag 4800, Christchurch 8020, New Zealand

⁵⁸IRAP, Université de Toulouse, CNRS, 14 Avenue Edouard Belin, 31400 Toulouse, France

⁵⁹UPMC-CNRS, UMR 7095, Institut d’Astrophysique de Paris, 98bis boulevard Arago, F-75014 Paris, France

⁶⁰Department of Physics, Massachusetts Institute of Technology, 77 Mass. Ave., Cambridge, MA 02139, USA

⁶¹Dept. of Earth, Atmospheric and Planetary Sciences, 54-1713, Massachusetts Institute of Technology, 77 Massachusetts Avenue, Cambridge, MA 02139, USA

⁶²European Southern Observatory, Casilla 19001, Vitacura 19, Santiago, Chile

⁶³McDonald Observatory, 16120 St Hwy Spur 78 #2, Fort Davis, Texas 79734, USA

⁶⁴Department of Physics, University of Rijeka, Omladinska 14, 51000 Rijeka, Croatia

⁶⁵Technische Universität Wien, Wieder Hauptst. 8-10, A-1040 Vienna, Austria

⁶⁶Perth Observatory, Walnut Road, Bickley, Perth 6076, WA, Australia

⁶⁷South African Astronomical Observatory, P.O. Box 9 Observatory 7925, South Africa

1. Introduction

High-magnification microlensing events provide a powerful tool for planet detection, partly because planets are more likely to perturb these events and partly because their high magnification (hence high signal-to-noise ratio) allows even very small perturbations to be detected. However, non-microlensing flux variations are also enhanced in these events. In this paper we report on the discovery of an apparent planet candidate that turned out instead to be a highly magnified active star and discuss methods by which we identified and excluded this interloper.

Stars are intrinsically variable, and star spots can induce substantial light curve variations in cool stars. However, for most G and K dwarfs this variability is manifested at a low level because magnetic activity decays quickly with age. Late M dwarfs can remain active for a Hubble time, but they are faint and will not be common microlensing sources. There is, however, an important sub-population of highly active RS CVn stars (Hall 1976) that are intrinsically luminous.

Magnetic activity is governed by the Rossby number (Noyes et al. 1984), $R_O \equiv P/t_c$, where P is the rotation period and t_c is the convective overturn timescale. Greater rotation (smaller P) induces faster buildup of magnetic fields. Deeper convection (bigger t_c) permits the fields to build up for a longer time before they propagate to the surface. In the R_O regime of interest here, the observed rms photometric variability A_r is a very steep function of $1/R_O$ (Hartman et al. 2009)

$$A_r \propto R_O^{-3.5 \pm 0.5}; \quad R_O \equiv \frac{P}{t_c}. \quad (1)$$

As stars leave the main sequence they will develop deep surface convection zones as they become cooler, but they will also be expand substantially and slow down due to angular momentum conservation. Hence, some special circumstance is required to induce or permit relatively rapid rotation. There are three potential mechanisms. First, a K dwarf may find itself in a close binary (either by birth, or through 3-body interactions), and thus be spun up by tides. Second, an F or G dwarf may find itself in a wider binary that is not initially tidally interacting. But as the dwarf evolves into a K subgiant, its expanding radius enables tidal interactions with its companion that then spin up the subgiant. Finally, stars in a narrow range of masses, $1.25 M_\odot \lesssim M \lesssim 1.5 M_\odot$ (typically F dwarfs) can spend most of their lives spinning fairly rapidly because of their shallow convection zones and so are still spinning

¹Based on observations made with the European Southern Observatory telescopes, Program ID 85.B-0399(I)

when they evolve into K subgiants. The lower mass limit is required for fast rotation to survive. Above the upper mass limit, stars evolve so rapidly through the Hertzsprung gap that they spend almost no time as subgiants. The resulting single-star RS CVn subgiants therefore span a narrow range of ages, $7 \text{ Gyr} \gtrsim t \gtrsim 3 \text{ Gyr}$.

Here we report the detection of the first spectroscopically confirmed RS CVn star in the Galactic bulge. The detection was beyond serendipitous. It resulted from intensive spectroscopic and photometric observations of an extremely rare high-magnification microlensing event of a subgiant source. Only about 1 bulge subgiant per 100 million is so magnified each year. The intensive photometry was carried out to find planets (orbiting the lenses), while the high-resolution spectrum of MOA-2010-BLG-523S was obtained to study chemical abundances of bulge dwarfs and subgiants.

MOA-2010-BLG-523S is a subgiant, with a temperature $T \sim 5123 \text{ K}$ and surface gravity $\log g = 3.6$ (Bensby et al. 2011, 2013)². As such, either the second or third mechanism of forming RS CVn stars should apply. That is, it is either in a binary that was “tidally activated” by the growth of the primary as it evolved along the subgiant branch, or it is an isolated, retired F dwarf. The mere existence of an isolated RS CVn star would be evidence for intermediate-age bulge stars. Of course, with just one detection, one could not make a reliable estimate of the fraction of bulge stars that are of intermediate age. But there are other lines of evidence for such a population, including age estimates of microlensed dwarfs and subgiants (Bensby et al. 2011) and asymptotic giant branch (AGB) stars (Cole & Weinberg 2002; van Loon et al. 2003; Uttenthaler et al. 2007). Thus, it would be of considerable interest to distinguish between the single-star and binary-star scenarios. Unfortunately, we find that both scenarios are plausible, given the available evidence, and so no definitive statement can be made regarding a putative intermediate-age population.

A major focus of the present paper is the secure identification of the microlensed subgiant as an RS CVn star. However, the process of this discovery is of independent scientific interest. The event became a focus of attention because of deviations from standard microlensing seen over the peak. The *I*-band lightcurve was quite well fit by a planetary model, and hence was far “along the road” to being published as a microlensing planet, in which case it would have been only the 14th such planet. It was really only very small discrepancies that led to the gradual unraveling of this picture and the recognition that the deviations

²The stellar parameters quoted in this work are taken from Bensby et al. (2013). These values are slightly revised from the ones originally given by Bensby et al. (2011). Because we discuss the history (Section 6) of how MOA-2010-BLG-523S was recognized to be an RS CVn star, we report here, for completeness, the Bensby et al. (2011) parameters that were available at that time: $T = 5250$, $\log g = 4.0$, $[\text{Fe}/\text{H}] = +0.1$, $\xi = 2.1 \text{ km s}^{-1}$.

at peak are most likely due to magnified star spots rather than a planet orbiting the lens star. The fact that irregular variability due to spots can be fit by planetary microlensing is sobering. As we discuss in Section 6, it implies that great care is required to securely identify microlensing planets in high-magnification events for cases of low-amplitude signals that lack clear microlensing signatures.

2. Observational Data

Microlensing event MOA-2010-BLG-523 (RA,Dec) = (17:57:08.9, $-29:44:58$) (l, b) = (0.59, -2.58) was alerted by the Microlensing Observations in Astrophysics (MOA) (Bond et al. 2001; Sumi et al. 2011) collaboration at UT 08:46, 21 Aug 2010, and again 26.5 hours later as a potential high-mag event that would peak at $A_{\max} \sim 70$ in four hours. In fact the event continued to rise for another 36 hours, which triggered much more intensive observations. At UT 16:51 23 Aug, the Microlensing Follow Up Network (μ FUN) issued a high-mag alert, predicting a peak at UT 02:00 to 04:00 and on this basis contacted the VLT bulge-dwarf spectroscopy group, advocating observations in that time interval. At the same time μ FUN organized its own continuous photometric observations using the 1.3m SMARTS telescope at CTIO to begin shortly after twilight. Very importantly in the present context, these observations were carried out with the ANDICAM camera, which is equipped with an optical/infrared dichroic, so that it can take images simultaneously in, e.g., I -band and H -band.

While the prediction of peak time turned out to be correct, VLT was unable to observe the event exactly when requested due to a conflict with technical activities, but did make a 2 hour exposure (split in 4x30-min) with UVES on VLT beginning near twilight (UT 23:56). The main information on this spectrum has already been reported by Bensby et al. (2011).

There are two other very important data sets coming from the Optical Gravitational Lens Experiment (OGLE) (Udalski et al. 1994; Udalski 2003). The event itself was monitored by OGLE-IV, which began operations in March 2010. However, during 2010, OGLE-IV was in commissioning phase and so did not issue alerts. The data were first reduced in November 2010. Unfortunately, the target falls in a gap between chips in the new 32-chip OGLE-IV camera, meaning that the target was captured only when small pointing errors moved the target onto a chip, which occurred about 1/3 of the time. Due to the high quality of OGLE data (and despite the reduced coverage), it was already evident that the source was a low-amplitude variable and indeed it was checked (and confirmed) at the time of the image reductions that these variations were not due to chip-edge effects. Hence, AU had already suggested at this time that “the analysis of this object may be more complicated than expected”.

The target also appears in OGLE-III, which took microlensing data from 2002-2009. And in addition, it was in a field that was the subject of a special high-cadence 46 day campaign in 2001 whose aim was to find transiting planets, during which it was observed 786 times.

In addition there were several other data sets, which in particular define the falling wing of the lightcurve extremely well. These include the RoboNet 2.0m Faulkes North Telescope (SDSS-*i*) in Hawaii, the PLANET 1.0m Canopus Telescope (*I*) in Tasmania (Australia), the PLANET 0.6m telescope (*I*) in Perth, Australia, and the following μ FUN telescopes: Auckland 0.4m (*I*), Farm Cove 0.36m (unfiltered), Kumeu 0.36m (*I*), Molehill 0.3m (unfiltered) (all in New Zealand), The 0.6m University of Canterbury B&C telescope intensively observed both wings of the light curve. Like the MOA 1.8m telescope, it is located at Mt. John, New Zealand. Finally the MiNDSTeP 1.5m telescope (*I*) in La Silla, Chile obtained data including a few points over the crucial peak region.

3. Microlensing Analysis (Simple Version)

As discussed in Section 6, a complete analysis of the microlensing event MOA-2010-BLG-523 is complicated by spots on the surface of the source (called MOA-2010-BLG-523S). However, it is possible to derive reasonably robust estimates of all the microlensing parameters required to constrain the source properties without detailed modeling of these complexities.

We begin by simply excising the data within 0.8 days of the peak and fitting the rest of the lightcurve flux F to the standard Einstein-Liebcs-Refsdal-Paczynski (1936, 1964, 1964, 1986) 5-parameter form

$$F(t) = f_s A(u[t]) + f_b; \quad u^2 = \frac{(t - t_0)^2 + u_0^2}{t_E^2}; \quad A = \frac{u^2 + 2}{u\sqrt{u^2 + 4}} \quad (2)$$

Here A is the magnification, u is the projected source-lens separation in units of the Einstein radius, u_0 is the impact parameter, t_0 is the time of closest approach, t_E is the Einstein crossing time, f_s is the source flux, and f_b is any blended flux that does not participate in the event but is within the same point spread function (PSF) as the source. If there is more than one observatory, then each requires its own (f_s, f_b) . We find

$$t_0 = 5432.603 \pm 0.002; \quad t_E = 18.5 \pm 0.5 \text{ day}, \quad u_0 \lesssim 0.002 \quad (3)$$

and for the OGLE observatory

$$I_s = 19.33 \pm 0.03; \quad \frac{f_b}{f_s} = 0.03 \pm 0.03. \quad (4)$$

(All times are given in HJD' = HJD-2450000).

Inspection of the relatively flat-peaked lightcurve shows that the lens crossed directly over the source and that the source crossing time is (crudely) of order $t_* \sim 0.15$ day, implying a source size (normalized to the Einstein radius) $\rho \equiv t_*/t_E \sim 0.008$. Hence, because $u_0 \ll \rho$, (and noting that $A \rightarrow u^{-1}$ for $u \ll 1$) we can approximate the peak predicted magnification as

$$A_{\max} = \langle r^{-1} \rangle \rightarrow \frac{2}{\rho} \left[1 + \left(\frac{3\pi}{8} - 1 \right) \Gamma \right] \quad (5)$$

where $\langle r^n \rangle$ is the n th moment of the source surface brightness, and where we have assumed a linearly limb-darkened (and unspotted) source in making the evaluation, in which case the moments can generally be evaluated

$$\langle r^n \rangle = \frac{\rho^n}{n/2 + 1} (1 - \alpha_n \Gamma); \quad \alpha_n = 1 - \frac{(3/2)!(1 + n/2)!}{(3/2 + n/2)!}. \quad (6)$$

Here Γ is the “natural” form of the linear limb-darkening coefficient, defined by surface brightness $S(r) \propto 1 - \Gamma[1 - (3/2)(1 - (r/\rho)^2)^{1/2}]$ (Albrow et al. 1999). It is related to the standard form u by $\Gamma = 2u/(3 - u)$. It is more “natural” in the sense that there is no net flux associated with the limb-darkening term, which results in simpler formulae when written in terms of Γ . This includes not just the moment equations (6), but all formulae without exception. For example, the limb-darkening term in the standard formula for ellipsoidal variation (Morris 1985), $(15 + u)/(3 - u)$ becomes simply $(5 + 3\Gamma)$.

We adopt $\Gamma_I = 0.477$ from Claret (2000), by applying the stellar parameters measured by Bensby et al. (2011): $T = 5123$ K, $[\text{Fe}/\text{H}] = +0.06$, $\log g = 3.6$, $\xi = 1.68 \text{ km s}^{-1}$. Hence, $A_{\max} = 2.17/\rho$. We evaluate A_{\max} by taking the ratio of observed flux at peak to the fit value of f_s , and get very nearly the same answer, whether using the average of the two OGLE peak points, or a median estimate of CTIO near-peak points: $A_{\max} = 265$. We thereby derive

$$\rho = 2.17/A_{\max} = 0.0082 \pm 0.0003 \quad (7)$$

where the error is derived from the 3% error in f_s and a 3% error in the peak flux due to spots.

4. Observational Properties of MOA-2010-BLG-523S

4.1. Baseline Variability

As we will argue below, the rms variability of the source is about 3%. This is to be compared with the photometric errors, which are typically close to 10%. If the source were

a strictly periodic variable, then the period could easily be identified by folding the light curve, despite the low signal-to-noise ratio (S/N) of individual points. The situation is more complex for a quasi-periodic variable (as would be expected for a rotating spotted star). We are therefore quite fortunate that the source lay in a 2001 OGLE transit-campaign field, which was observed 786 times on 32 separate nights during a 46-day window. Binning the data by day, we therefore achieve errors of 0.02, which is comparable to the amplitude of the signal. The result is shown in Figure 1. The lightcurve gives the clear impression of variability with a period of order 12 days.

We then use all the OGLE-III data to test for a quasi-periodic signal. If this is a spotted star, we expect that the underlying physical mechanism (rotation of the star) will be strictly periodic, but that the phase of the variations will drift over time as spots appear and disappear. As discussed above, except during the transit campaign, we are compelled to fold the data to pick up any signal at all. On the other hand, if we fold data over an interval that is too long, the result will suffer from destructive interference between different phase regimes. We therefore consider separate fits to the data for each of the nine seasons, 2001-2009. In each trial, we hold the period fixed at a common value for all seasons. Hence, there are 28 parameters [Period + $9 \times (\text{phase, amplitude, zero-point})$]. At $P = 10.914 \pm 0.055$ days, there is an improvement of $\Delta\chi^2 = 69$ relative to a fit for constant magnitude in each season (9 parameters), i.e., 19 fewer parameters. See Figure 2.

We find that the phases are not consistent from one season to the next, suggesting that the variations are not strictly periodic. To further test this, we fit for a single phase and amplitude together with a zero-point offset for each season. This produces an improvement (relative to no periodic variations) of only 30 for 3 dof. Clearly the quasi-periodic variations are favored over strictly-periodic variations.

4.2. Source is the Variable

Faint sources in crowded fields are usually blends of several stars rather than discrete sources. And, of course, for microlensing events there is guaranteed to be at least one additional star along the line of sight in addition to the source, namely the lens. Hence, observing baseline variations does not in itself prove that the source is variable. However, from the microlens fit presented in Section 3, we know that the blend is at least 15 times fainter than the source. Thus, if it were responsible for the $\sim 3\%$ variations seen at baseline, it would itself have to vary at the $\gtrsim 50\%$ level on ~ 11 day timescales. Such stars are extremely rare. Moreover, the chance is remote that one of these would happen to align with a source that (from other evidence we will present below) is expected to be variable.

Therefore we conclude that it is MOA-2010-BLG-523S that is varying.

4.3. Calcium H&K Emission

Figure 3 shows the region of the calcium H&K lines in the UVES spectrum taken by Bensby et al. (2011) near the peak of the event. The emission is extremely strong. We measure $S_{\text{HK}} = 0.79 \text{ \AA}$ by taking the ratio of the flux in these lines to the mean “continuum” in the neighboring “V” and “R” regions (see Fig. 3). For comparison Isaacson & Fischer (2010) found only 3 cases of comparable or larger S_{HK} among 234 “subgiants” in their survey of field stars. See their Figures 11 and 12. We will discuss these in Section 5.3 below, but for the moment note that the Isaacson & Fischer (2010) stars are substantially redder and more luminous than MOA-2010-BLG-523S.

4.4. Microturbulence Parameter ξ

Figure 4 shows the microturbulence parameter ξ plotted against temperature for 26 microlensed dwarfs and subgiants as found by Bensby et al. (2010, 2011). MOA-2010-BLG-523S has one of the largest ξ . Moreover, it is well above the upper envelope of points on the low-temperature part of the diagram. This high “microturbulence” may reflect real turbulent motions on the surface of the star (as would be expected for an active star), but may in part reflect rotational motion. Since microturbulence represents a Gaussian velocity distribution that adds to line is quadrature with other effects, like instrumental resolution, unmodeled rotational motion will contribute to ξ as

$$\Delta\xi^2 = \frac{\langle r^2 \rangle}{\langle r^0 \rangle} \frac{(v \sin i)^2}{2} = \frac{1 - 0.2\Gamma}{4} (v \sin i)^2 \quad (u \gg \rho) \quad (8)$$

where $v \sin i$ is the projected rotational motion.

In fact, Equation (8) applies to sources that are not differentially magnified, which is of course the usual case, but not the present one. If the lens were directly aligned with the source, then

$$\Delta\xi^2 = \frac{\langle r^1 \rangle}{\langle r^{-1} \rangle} \frac{(v \sin i)^2}{2} \simeq \frac{1 - 0.3\Gamma}{6} (v \sin i)^2 \quad (u = 0). \quad (9)$$

i.e., roughly 2/3 of the non-differentially magnified case. For the actual geometry at the time of VLT spectra and I -band limb-darkening, we find below that $\Delta\xi^2 = 0.2(v \sin i)^2$. Hence the measured ξ places an upper limit on $v \sin i$,

$$v \sin i \lesssim \sqrt{5}\xi = 3.8 \text{ km s}^{-1} \quad (10)$$

4.5. Lithium

In principle, it is possible to produce an isolated rapidly spinning subgiant (hence, an isolated RS CVn star) in an old population via stellar mergers. For example, a 10-Gyr solar mass star could begin evolving off the main sequence and swallow a smaller star, say $0.3 M_{\odot}$, that had been its companion. This would both spin up the cannibal and provide fresh fuel to extend its life. The mass would be raised above the break in the Kraft (1970) curve, so that the star would not substantially spin down during its extended life. It would then evolve along the subgiant branch in a manner similar to any other $1.3 M_{\odot}$ star. However, this scenario is ruled out in the present case because Bensby et al. (2011) detected lithium with abundance $\log \epsilon(\text{Li}) = 1.6$. Essentially all lithium would have been destroyed if there had been a stellar collision (Hobbs & Mathieu 1991; Andronov et al. 2006). Thus, if MOA-2010-BLG-523S could be shown to lack companions, it would be of intermediate age.

4.6. Radial Velocity

The fraction of microlensing events toward the bulge whose source stars lie in the bulge (as opposed to the foreground disk) is $\gtrsim 95\%$. This is primarily because the optical depth to lensing is much higher due to the higher column of lenses. But this effect is also compounded by the fact that there are simply more bulge sources in these fields compared to disk stars. Nevertheless, if a source is weird in some way, its weirdness may be intrinsically connected with it being one of the small fraction of disk sources. This possibility is especially relevant in the present case because the disk is known to harbor a population of youngish subgiants, whereas the bulge is not.

The source radial velocity (RV), $v_r = +97.3 \text{ km s}^{-1}$ (Bensby et al. 2011), makes it highly unlikely that it is in the disk because the expected value for disk stars is $v_{r,\text{disk}} = +10 \pm 34 \text{ km s}^{-1}$ (compared to $+10 \pm 100 \text{ km s}^{-1}$ for the bulge).

4.7. Source Size

Bensby et al. (2011) derive an equivalent $(V - I)_0 = 0.86$ color from their spectroscopic solution (primarily from the temperature, but also taking account of the metallicity and gravity). We find from the microlens solution in Section 3 that the unmagnified source flux is $\Delta I = 3.18$ mag fainter than the clump. From the color-magnitude diagram of the neighboring field, there appears to be very little differential reddening. Hence $\Delta I \simeq \Delta I_0$. Based on the measured metallicity distribution of bulge stars, Nataf et al. (2012) estimate that the

absolute magnitude of the clump is $M_{I,\text{cl}} = -0.12$. Therefore, the absolute magnitude of the source is

$$M_{I,s} = M_{I,\text{cl}} + \Delta I - 5 \log \frac{D_s}{D_{\text{cl}}} = 3.06 - 5 \log \frac{D_s}{D_{\text{cl}}} \quad (11)$$

where the last term is the ratio of the distances to the source and the clump. We then apply standard techniques (Yoo et al. 2004) to evaluate the source radius, first using Bessell & Brett (1988) to convert $(V - I) \rightarrow (V - K)$ and then using Kervella et al. (2004) to obtain the K -band surface brightness from the $(V - K)$ color. Finally, we find

$$R_s = 2.15 R_\odot \frac{D_s}{D_{\text{cl}}}. \quad (12)$$

Note in particular that this derivation is independent of any assumption about the Galactocentric distance R_0 or the geometry of the Galactic bar, etc. Subgiants would be expected to have $R_s \gtrsim 2 R_\odot$. Hence, the source cannot lie substantially closer than the bulge because it would then be too small to be a subgiant (as indicated by its spectroscopic gravity).

4.8. Consistency of Spectrum with Stellar Rotation

If the source is rotating with a period $P = 10.9$ days, as seems indicated by the quasi-periodic variability seen in Figures 1 and 2, then the surface velocity is $v = 2\pi R_s/P = 10.0 \text{ km s}^{-1} (R_s/2.15 R_\odot)$. The upper limit $v \sin i \lesssim 3.8 \text{ km s}^{-1}$ (Eq. [10]) then implies $i \lesssim 22^\circ$. This is a plausible value since randomly oriented stars will be uniformly distributed in $\cos i$. That is, 7% of stars have $i < 22^\circ$, which is small but not implausibly so.

4.9. Consistency with Maoz-Gould Effect

Maoz & Gould (1994) predicted that microlensing of rotating stars would generate an apparent RV shift, which would change during the course of the event. Their principal point was that the magnitude of this effect falls off only linearly with relative source-lens separation $z \equiv u/\rho$, compared to the quadratic fall-off of photometric effects:

$$\Delta v = \frac{\langle r^2 \rangle}{\langle r^0 \rangle} \frac{v \sin i}{2z} \sin \phi = \frac{1 - 0.2 \Gamma}{4z} v \sin i \sin \phi \quad (z \gg 1) \quad (13)$$

where ϕ is the angle between the source-lens separation and the projected spin axis.

The Bensby et al. (2011) spectrum is actually composed of 4 30-minute exposures, centered on $\text{HJD} - 2455432 = (0.510, 0.531, 0.552, 0.573)$. Because the lens came very close to

source center, we will adopt $z = (t - t_0)/t_*$. As we discuss in Section 6, t_0 is not very accurately predicted by the lightcurve with the peak data removed and is actually approximately $t_0 = 5432.66$ (compared to $t_0 = 5432.60$ found in Section 3). Therefore, at the four epochs, $z = (1.00, 0.86, 0.72, 0.58)$. We find numerically that the pre-factor in Equation (13) at these four epochs is $(0.294, 0.333, 0.311, 0.266)$. Thus, the maximum predicted relative shift is only $0.067v \sin i \sin \phi < 0.31 \text{ km s}^{-1}$. Based on cross correlation, the four spectra are consistent at this level.

5. Possible Local Analogs

We search for local analogs of MOA-2010-BLG-523S in order to better understand its nature and, to this end, begin by summarizing its characteristics.

5.1. Summary of Characteristics

From Bensby et al. (2011, 2013), we know the temperature, iron abundance, gravity, microturbulence, and lithium abundance: $T = 5123 \pm 98 \text{ K}$, $[\text{Fe}/\text{H}] = 0.06 \pm 0.07$, $\log g = 3.60 \pm 0.23$, $\xi = 1.68 \pm 0.20$, $\epsilon(\text{Li}) = 1.64 \pm 0.10$. Bensby et al. (2011) also remark that the source has high sodium, which they note could be “fixed” by making it 500K hotter or increasing $\log g$ by 1 dex. However, they investigate these possibilities and reject them. While Bensby et al. (2011) did not take account of differential magnification in their analysis, the impact of such differential magnification is quite small. For example, “Profile 35” considered by Johnson et al. (2010) had much stronger differential magnification, but this affected the temperature by only 20K (see their Figs. 3 and 8).

The baseline variability analyzed in Section 4.1 is best modeled as having constant period $P = 10.914$ days, but variable phase over 9 years, as would be predicted for a spotted star. We find variability amplitudes in these seasons (in mmags) of 20 ± 4 , 40 ± 8 , 25 ± 10 , 26 ± 9 , 53 ± 9 , 28 ± 7 , 13 ± 10 , 27 ± 9 , 83 ± 19 . Hence, a median of 0.027 mag, implying an rms variability of 2%. This is actually a lower limit, since each season’s variability measure can be impacted by destructive interference between spot cycles at different phases.

Finally, in Section 4.3, we measured calcium H & K emission of $S_{\text{HK}} = 0.79 \text{ \AA}$.

5.2. Comparison by Rossby Number to M37 Sample

From stellar models, we find that the convective overturn timescale for a $T = 5123\text{K}$ subgiant is 3 times longer than for the Sun, while the measured period is 2.3 times shorter. Hence the Rossby number is 7 times higher. From Figure 17 of Hartman et al. (2009), we observe that stars in M37 with similar $R_O \simeq 0.3$ have rms variability in the range of 1–6%. Hence, the observed variability is quite consistent with locally observed stars.

5.3. Comparison to Isaacson & Fischer Sample

As discussed in Section 4.3, Isaacson & Fischer (2010) found only three stars with comparable or greater S_{HK} in their sample of 234 subgiants. These are Hipparcos stars HIP 5227, 8281, and 97501, which have $(V - K) = 2.43, 2.56, 2.59$. They are thus considerably redder than MOA-2010-523S, which has $(V - I)_0 = 0.86$ estimated from its spectrum (Bensby et al. 2011), corresponding approximately to $(V - K)_0 = 1.92$. They are also about 1–1.5 mag more luminous than the subgiants in the Bensby et al. (2011) sample shown in Figure 4. Indeed stars of this color and luminosity would not be deliberately selected for the Bensby et al. (2011) “dwarf and subgiant” program, and are excluded from the analysis if they are observed by accident (Johnson et al., in prep). Based on their V/K photometry, Hipparcos distances, combined with the Kervella et al. (2004) surface brightness relations, these three stars have radii of 5.4, 5.9, and 7.0 R_\odot , respectively.

All three of these stars are spectroscopic binaries and at least the first two are broadly consistent with being tidally synchronized. Their binary periods are respectively 27.3 and 30.1, days (Eker 2008), which would imply surface velocities of 10 km s^{-1} in both cases, while Isaacson & Fischer (2010) report $v \sin i$ of 14 and 6.2 km s^{-1} , respectively. However, D. Fischer (2011, private communication) notes that the profile of the first star is contaminated by lines from a companion, which she estimates to broaden the $v \sin i$ determination by 20–30%, making both stars quite consistent with tidal synchronization. D. Fischer also notes that the third star (Hip 97501) is a clear double-lined spectroscopic binary, so that its binary nature is not in doubt even though the 3 RV measurements by Isaacson & Fischer (2010) show a scatter of only 0.2 km s^{-1} .

A plausible scenario for these stars is that their moderately close companions only started to spin them up when they began to expand their envelopes as they approached the giant branch. In particular, for the first two, their known periods ($P \sim 30$ days) are too long for tidal synchronization while the stars were on the main sequence. However, as they evolved along the subgiant branch, they were clearly tidally spun up, as evidenced both by

their $v \sin i$ and their calcium H & K activity.

Because MOA-2010-BLG-523S is a much smaller star, a much closer companion would be required to tidally couple with it. On the other hand, its period is much shorter. Since tidal amplitudes scale $\propto R^3/P^2$, a companion in an 11 day period could provide tidal interactions only a factor ~ 2 smaller than these local analogs. Because MOA-2010-BLG-523S’s period is shorter and its phase of subgiant evolution is longer, it would have many more periods to tidally synchronize. Hence, tidal spin-up by a binary companion is a very plausible explanation for its variability and the strength of its calcium lines.

5.4. Comparison to *Kepler* Sample

Chaplin et al. (2011) find a dramatic drop in the interval $5150\text{K} < T < 5400\text{K}$ in the fraction of *Kepler* asteroseismology targets for which they can measure oscillations. These show variability in the range 0.1–10 mmag, which is modestly higher than neighboring temperature ranges. See their Figure 1. The most plausible interpretation is that subgiants in this temperature range preferentially acquire spots that physically interfere with the propagation of stellar oscillations. (Oscillations in dwarf stars at these temperature ranges would be undetectable in any case.) This cannot be due to close binary companions because the phenomenon is nearly universal, whereas only a few percent of stars have such close companions. Rather, the physical mechanism must be that as single stars evolve redward on the giant branch, their convection zones deepen, so t_c increases, and they become more spotted. After they pass through the most-affected temperature range, they expand rapidly, thus increasing their moment of inertia and so slowing their rotation. Of course, the more rapidly they are rotating at the outset, the higher the level of activity, but the increase in activity at this temperature range is nearly universal.

Because the temperature $T = 5123\text{K}$ of MOA-2010-BLG-523S is at the edge of this affected range, it is also a plausible candidate to be a non-binary active subgiant.

6. Birth and Death of a Microlens “Planet”

Due to its predicted high-magnification, MOA-2010-BLG-523 was monitored almost continuously over peak by the 1.3m SMARTS telescope, although there were short gaps to check on another, possibly interesting, event. These data, by themselves, display a significant “bump” near peak. Moreover, the time of the observed peak is asymmetrically offset from that expected based on the MOA data (roughly a half day on either side of peak) by about

1.5 hours. Such bumps and asymmetries are just the type of features we look for to identify planetary anomalies due to central caustics in high-magnification events. Within 2 days, preliminary models were circulated and within 4 days, a planetary model was found that matched all the major lightcurve features. See Figure 5.

In accord with standard microlensing practice, one person (JCY) was assigned to systematically review all the evidence and propose a final model, which would then be vetted by all groups contributing data. Her report stated that the observed deviations were most likely due to either systematics in the data or stellar variability and so most likely implied that there was no planet or, in any case, that it was impossible to reliably claim a planet. Note that none of the evidence presented here that MOA-2010-BLG-523S is an RS CVn star entered into JCY’s reasoning or report.

Rather, JCY was led to question the planetary model because of three features. First, the model source crossing time was almost exactly half the naive time derived from inspection of the lightcurve. To enable this, the model has the source pass the planet-star axis almost exactly at right angles, so that it passes the middle (weak) cusp almost exactly at peak. See Figure 5. Second, one of the three predicted features of the peak lightcurve takes place in a small gap in the data. Third, another feature is somewhat more pronounced in the model than in the data. Each of these is, by itself, quite plausible and within the range of microlensing experience, but together were suspicious.

Hence, JCY sought confirmation of the planetary signal in other data sets. Unfortunately, the two other Chile observatories that might have taken such data (OGLE and La Silla) had very sparse coverage. She therefore investigated the CTIO ANDICAM *H*-band data, which are normally of substantially lower quality than the *I*-band data and so are usually used only for special purposes, such as comparison with high-resolution post-event *H*-band imaging (e.g., Janczak et al. 2010) or when *I*-band data are saturated (e.g., Dong et al. 2009). In this case, the *H*-band data showed a smooth peak, which is clearly inconsistent with the “bump” seen in *I*-band. See Figure 6. (Note, however, that the *H*-band peak is still asymmetrically offset by 1.5 hours compared to the time expected based on data in the wings.)

It is in principle possible to have “sharper” features in *I*-band than *H*-band due to limb-darkening effects. This is contrary to the general expectation that microlensing is achromatic since in general relativity geodesics do not depend on wavelength. This exception occurs when the lens resolves the source because limb darkening is more severe in bluer passbands making the light profile more compact. Nevertheless, the amplitude of the difference seen in this event is much too big to be explained by this effect. The relative difference in effective

source sizes is

$$\sqrt{\frac{\langle [r(H)]^2 \rangle}{\langle [r(I)]^2 \rangle}} - 1 = \sqrt{\frac{1 - 0.2\Gamma_H}{1 - 0.2\Gamma_I}} - 1 \sim 0.1(\Gamma_I - \Gamma_H) < 0.02 \quad (14)$$

whereas the difference in timescales of the observed deviations is a factor ~ 2 . Hence, there is no plausible reason for the difference in I and H band over the peak. Moreover, JCY found that the other part of the “planetary signal”, the asymmetry in the lightcurve (both I -band and H -band), can be fit by “xallarap” (orbital motion of the source about a companion) with periods of 3–15 days.

The path to gathering the evidence summarized in Section 4 was circuitous. First, in response to JCY’s report, AU reiterated that the source (or at least some star in the aperture) was a variable with an 11 day period and a 1% amplitude. This variability had previously been ignored in the analysis due to the fact that the “planetary” deviation had a much shorter timescale. Then AG learned from stellar-interiors expert MHP that RS CVn stars were found very frequently at $T \sim 5250$ K. MHP then suggested that the Rossby number scalings from Hartman et al. (2009) could explain the observed variability. In the meantime, it was found that variability at fixed period but random phase (characteristic of spots) is strongly favored over a strictly periodic signal. These results were consistent with an RS CVn star, so one would expect to see the strong calcium H & K emission characteristic of such stars in the UVES spectrum. However, Bensby et al. (2011) had not remarked upon this because the blue spectral channel is rarely if ever examined for stars in this program because they are very heavily reddened. A check of the blue channel indeed showed strong H & K lines. These lines proved to be easily detectable in this case not only because they are intrinsically strong, but also because the spectrum was taken at $I \sim 13.3$, which is substantially brighter than is typical for the Bensby et al. (2011) sample (see their Fig. 1).

In brief, the contradiction between the optical and IR lightcurves proved to be the crucial turning point in debunking the “planet”, even though a more detailed investigation of the available data provides overwhelming evidence that this was a microlensed RS CVn star.

This history argues for caution in the interpretation of planetary signals, particularly when they are both of small amplitude and without the discontinuous slopes characteristic of caustic crossings (e.g., Gould et al. 2006). One may counter in this case that RS CVn stars are extremely rare, but the fact remains that this “rare event” occurred within the first dozen or so microlensing planets. Such rare events in small samples remind us to be vigilant about our assumptions.

We note that the misinterpretation of microlensed spots as planetary signals was sug-

gested more than a decade ago by Heyrovský & Sasselov (2000), who specifically cautioned on the difficulty of distinguishing spots from planets in high-magnification events and even suggested intensive multi-band photometry as a means to tell the difference. As they remarked, such multi-band (optical/IR) photometry had already been advocated by Gaudi & Gould (1997) as a means to better characterize planetary perturbations. This earlier paper (see also Gould & Welch 1996) was the motivation to build the optical/IR dichroic camera ANDICAM (DePoy et al. 2003), whose I/H observations of MOA-2010-BLG-523 proved crucial in demonstrating that the deviations were due to spots rather than a planet. There were several other early investigations of the interpenetration of spots and binary or planetary microlensing. Han et al. (2000) argued that spots might be easier to study in binary-lens than single-lens microlensing because the caustics were more likely to transit the source. And Rattenbury et al. (2002) made a broader investigation of whether spots could in fact be mistaken for planets, arguing that this was really only possible in the rare events (such as MOA-2010-BLG-523) in which the lens passes very close to or over the source. However, to our knowledge, there are no previously published observations of microlensed spots.

7. RS CVn Stars in the Galactic Bulge

As we have emphasized, it will be quite rare that an RS CVn star is magnified sufficiently to get a high S/N spectrum of the heavily extincted Ca H & K lines. Nevertheless, there are other paths toward identifying bulge RS CVn stars. Udalski et al. (2012) found optical counterparts to X-ray sources from the Jonker et al. (2011) Galactic Bulge Survey (GBS) catalog, including 81 spotted stars, which are very probably RS CVn stars. However, because the underlying X-ray catalog is confined to $1 < |b| < 2$, it is likely that a large fraction of these are in the disk.

There are two relatively straightforward ways to distinguish between bulge and disk membership. First, a subset of seven of these 81 stars are eclipsing. All but one of these are relatively bright $12.7 < I < 15.2$, and so it should be possible to obtain spectra and thus measure their distances using the method of eclipsing binaries. Even the faintest of these, at $I = 17.4$, is not beyond reach. A large fraction of the remainder could be put on a clump-centric color magnitude diagram (Nataf et al. 2011). In most cases, this should clearly distinguish between bulge and foreground stars. Unfortunately, the extinction map of Nataf et al. (2012) does not reach most of the Udalski et al. (2012) stars because this map is based on OGLE-III data, whereas the GBS survey is restricted to low-latitude fields that are only covered by OGLE-IV. However, it should be possible to apply the clump-centric method to these OGLE-IV fields as well.

8. Conclusions

The evidence presented in Sections 4 and 5 that MOA-2011-BLG-523S is an RS CVn star is overwhelming. This star shows quasi-periodic variations (the form expected for spots) with a period of $P = 10.9$ days. The amplitude of variation (few percent) is consistent with what one would expect from its inferred Rossby number. It exhibits very strong calcium H & K emission, such as is seen in only 3 out of a sample of 234 local subgiants. All three are spectroscopic binaries, and two are known to have periods of $P \sim 30$ days, which given their radii and measured $v \sin i$ implies that they are tidally spun up. MOA-2010-BLG-523S has high microturbulence measured compared to the 26 microlensed dwarfs and subgiants, particularly among stars of similar temperature.

Unfortunately, it is not possible to say definitively whether MOA-2010-BLG-523S is in a binary or not. Its period relative to its radius is suggestive of being in the same class of tidally spun up binaries that includes the 3 calcium-active subgiants just mentioned. But its temperature is near the range of active subgiants found from Kepler seismology, the great majority of which must be single stars (or widely separated, non-interacting binaries). If a strong case could be made that this was not a binary, then from the lithium measurement (Section 4.5) this would be evidence for an intermediate age population. But this is not the case. The fact that the peak is offset from the time expected from the wings by 1.5 hours strongly suggests “xallarap” (orbital motion of the source due to a binary companion). However, the irregular character of the lightcurve, probably due to microlensed spots, compromises our ability to make a rigorous microlensing fit for xallarap.

The I -band lightcurve is well fitted by a planetary-lens model. The path to discovering that this is a coincidence, and that the lightcurve anomaly is due to spots was quite circuitous, as described in Section 6. This argues for caution in the interpretation of planetary microlensing events in which the deviations are small and lack features that are obviously due to a 2-body lens.

AG and JCY acknowledge support from NSF AST-1103471. Work by JCY was supported by an SNSF Graduate Research Fellowship under Grant No. 2009068160. AG, BSG, L-WH, and RWP acknowledge support from NASA grant NNX12AB99G. Work by C. Han was supported by Creative Research Initiative Program (2009-0081561) of National Research Foundation of Korea. TB was funded by grant No. 621-2009-3911 from The Swedish Research Council. Work by S. Dong was performed under contract with the California Institute of Technology (Caltech) funded by NASA through the Sagan Fellowship Program. Work by B. Shappee and J. van Saders were supported by National Science Foundation Graduate Research Fellowships. The MOA project acknowledges grants 20340052 and 22403003 from

JSPS. T. Sumi acknowledges support from JSPS23340044. The OGLE project has received funding from the European Research Council under the European Community’s Seventh Framework Programme (FP7/2007-2013) / ERC grant agreement no. 246678 to AU. MH acknowledges support by the German Research Foundation (DFG). DR (boursier FRIA) and J. Surdej acknowledge support from the Communauté française Belgique Actions de recherche concertées – Académie universitaire Wallonie-Europe. CS received funding from the European Union Seventh Framework Programme (FP7/2007-2013) under grant agreement 268421. The Danish 1.54 m telescope is operated based on a grant from the Danish Natural Science Foundation (FNU). KA, DMB, MD, KH, MH, CL, CS, RAS and YT would like to thank the Qatar Foundation for support from QNRF grant NPRP-09-476-1-078.

REFERENCES

- Albrow, M. et al. 1999, *ApJ*, 522, 1022
- Andronov, N., Pinsonneault, M.H., & Terndrup, D.M. 2006, *ApJ*, 646, 1160
- Bessell, M. S., & Brett, J. M. 1988, *PASP*, 100, 1134
- Bensby, T., et al. 2010, *A&A*, 512, 41
- Bensby, T., et al. 2011, *A&A*, 533, 134
- Bensby, T., et al. 2013, in prep
- Bond, I.A., et al. 2001, *MNRAS*, 327, 868
- Claret, A. 2000, *A&A*, 363, 1081
- Chaplin, W.J., et al. 2011, *ApJ*, 732, L5
- DePoy, D.L. et al. 2003, *SPIE* 4841, 827
- Duncan, D.K. 1991, *ApJS*, 76, 383
- Cole, A.A. & Weinberg, M.D. 2002, *ApJ*, 574, L43
- Dong, S., et al. 2009b, *ApJ*, 698, 1826
- Einstein, A. 1936, *Science*, 84, 506
- Eker, Z., et al. 2008, *MNRAS*, 389, 1722

- Gaudi, B.S. & Gould, A. 1997 ApJ, 486, 85
- Gould, A. & Welch, D.L. 1996, ApJ, 464, 212
- Gould, A., et al. 2006, ApJ, 644, L37
- Hall, D.S. 1976, in ASSL Vol. 60: IAU Colloq. 29: Multiple Periodic Variable Stars, ed. W.S. Fitch (Dordrecht: Reidel), 287
- Han, C., Park, S.-H., Kim, H.-I. & Chang, K. 2000, MNRAS, 316, 665
- Hartman, J.D., et al. 2009, ApJ, 691, 342
- Heyrovský, D. & Sasselov, D. 2000, ApJ, 528, 995
- Hobbs, L.M., & Mathieu, R.D. 1991, PASP, 103, 431
- Isaacson, H. & Fischer, D. 2010, ApJ, 725, 875
- Janczak, J. et al. 2010, ApJ, 711, 731
- Jonker, P.G., et al. 2011, ApJS, 194, 18
- Johnson, J.A. Dong, S., & Gould, A. 2010, ApJ, 713, 713
- Kervella, P., Thévenin, F., Di Folco, E., & Ségransan, D. 2004, A&A, 426, 297
- Kraft, R. 1970 in Spectroscopic Astrophysics, ec. G.H. Herbig (Berkeley: University of California Press), p. 385
- Liebes, S. 1964, Physical Review, 133, 835
- Maoz, D. & Gould, A. 1994, ApJ, 425, L67
- Morris, S.L. 1985, ApJ, 295, 143
- Nataf, D., Udalski, A., Gould, A., & Pinsonneault, M.H. 2011, ApJ, 730, 118
- Nataf, D. et al. 2012, ApJ, submitted, arXiv1208.1263
- Noyes, R.W., Hartmann, L.W., Baliunas, S.L., Duncan, D.K., & Vaughan, A.H. 1984, ApJ, 279, 763
- Paczynski, B. 1986, ApJ, 304, 1
- Rattenbury, N.J., Bond, I.A., Skuljan, J., & Yock, P.C.M. 2002, MNRAS, 335, 159

Refsdal, S. 1964, MNRAS, 128, 295

Sumi, T. et al. 2011, Nature, 473, 349

Udalski, A., Szymanski, M., Kaluzny, J., Kubiak, M., Mateo, M., Krzeminski, W., & Paczynski, B. 1994, Acta Astron., 44, 317

Udalski, A. 2003, Acta Astron., 53, 291

Udalski, A., Kowalczyk, K, Soszyński, I., et al. 2012, Acta Astron. 62, 133

Uttenthaler, S., Hron, J., Lebzelter, T., Busso, M., Schultheis, M., & Kufl, H.U., 2007, A&A463, 251

van Loon, et al., J.T. 2003, MNRAS, 338, 857

Yoo, J. et al. 2004, ApJ, 603, 139

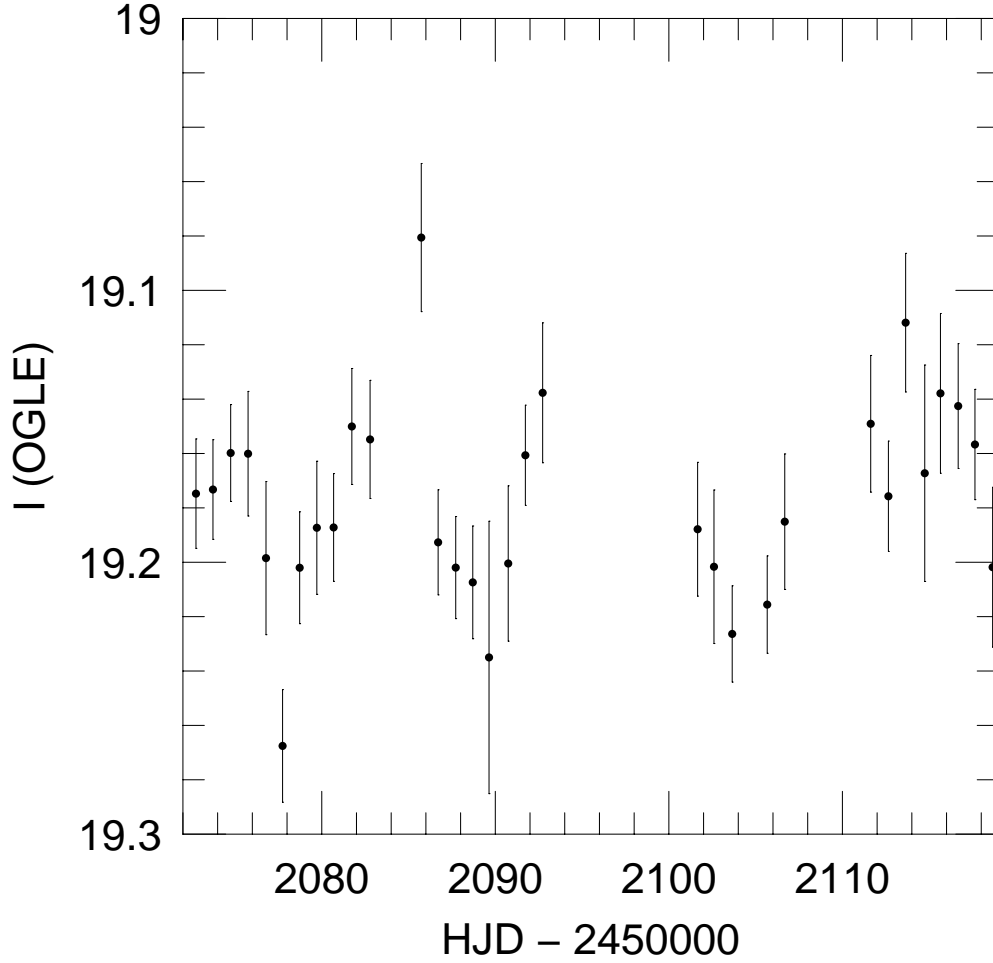


Fig. 1.— Lightcurve of MOA-2010-BLG-523S from the 2001 high-cadence OGLE transit campaign, binned by day. There are a total of 786 observations on 32 nights, spread over a 46 day interval. The underlying data have typical errors of 0.10 mag unbinned, hence 0.02 mag when binned. The source shows periodic or quasi-periodic oscillations with a period of roughly 12 days.

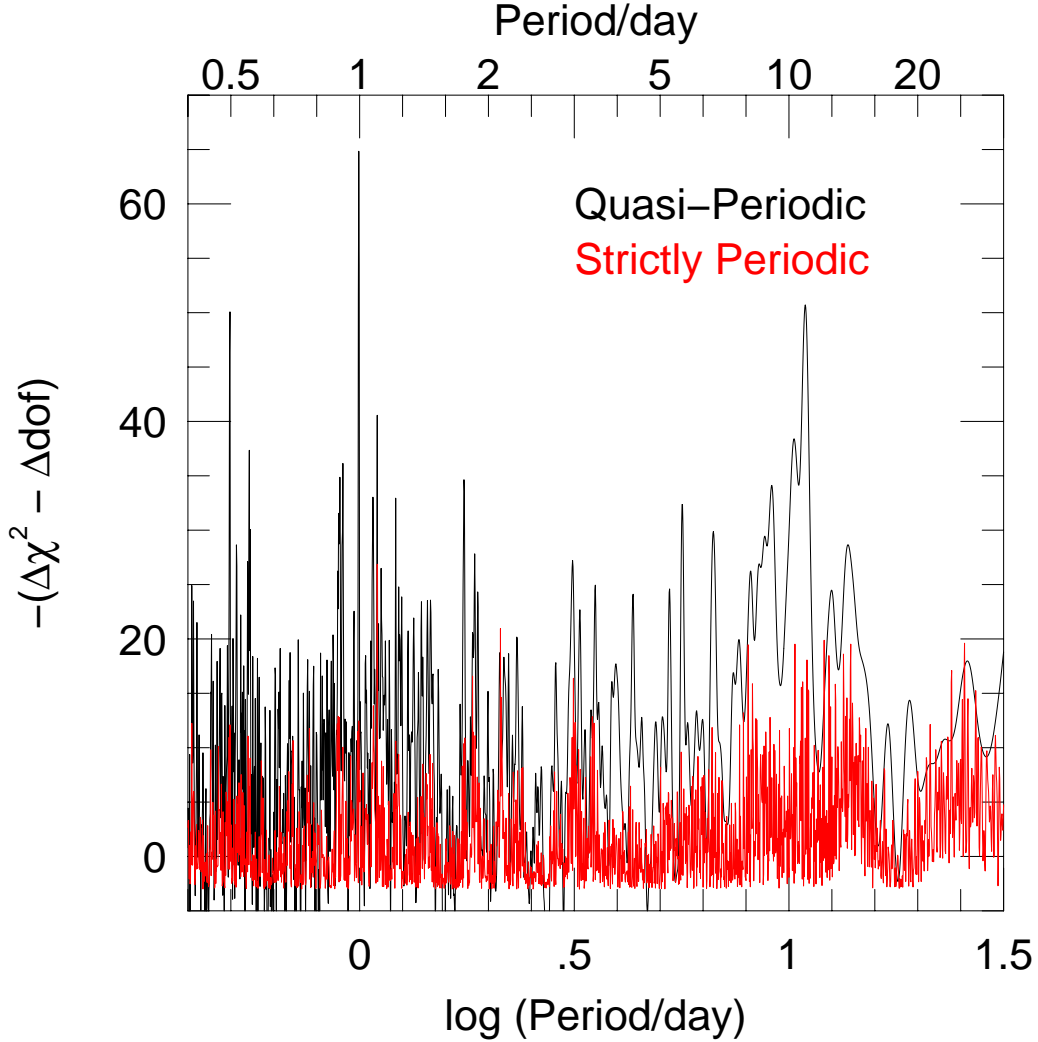


Fig. 2.— Goodness of fit of strictly periodic (red) and quasi-periodic (black) models of variability of MOA-2010-BLG-523S over nine OGLE-III seasons (2001-2009). The strictly periodic models have 12 free parameters (period, amplitude, phase, plus zero-point offsets for each season), while the quasi-periodic models have 28 (additional phases and amplitudes for each season). The ordinate shows the difference in χ^2 relative to a model with 9 parameters (zero-point offset at each season), [$\chi^2 = 2686.75$ for 2531 dof], taking account of the different number of dof. Except for a spike very close to 1 day (0.9947 ± 0.0005 day) the highest peak is at $P_0 = 10.914 \pm 0.055$ day. The quasi-periodic models are clearly favored over the strictly-periodic ones. Other notable peaks are at the alias of the sampling frequency (0.5 day), and at the aliases of the main peak, $P_{\pm} = 1/(1/P_0 \pm 1/\text{Day}_{\text{synod}}) = (0.913, 1.098)$ day.

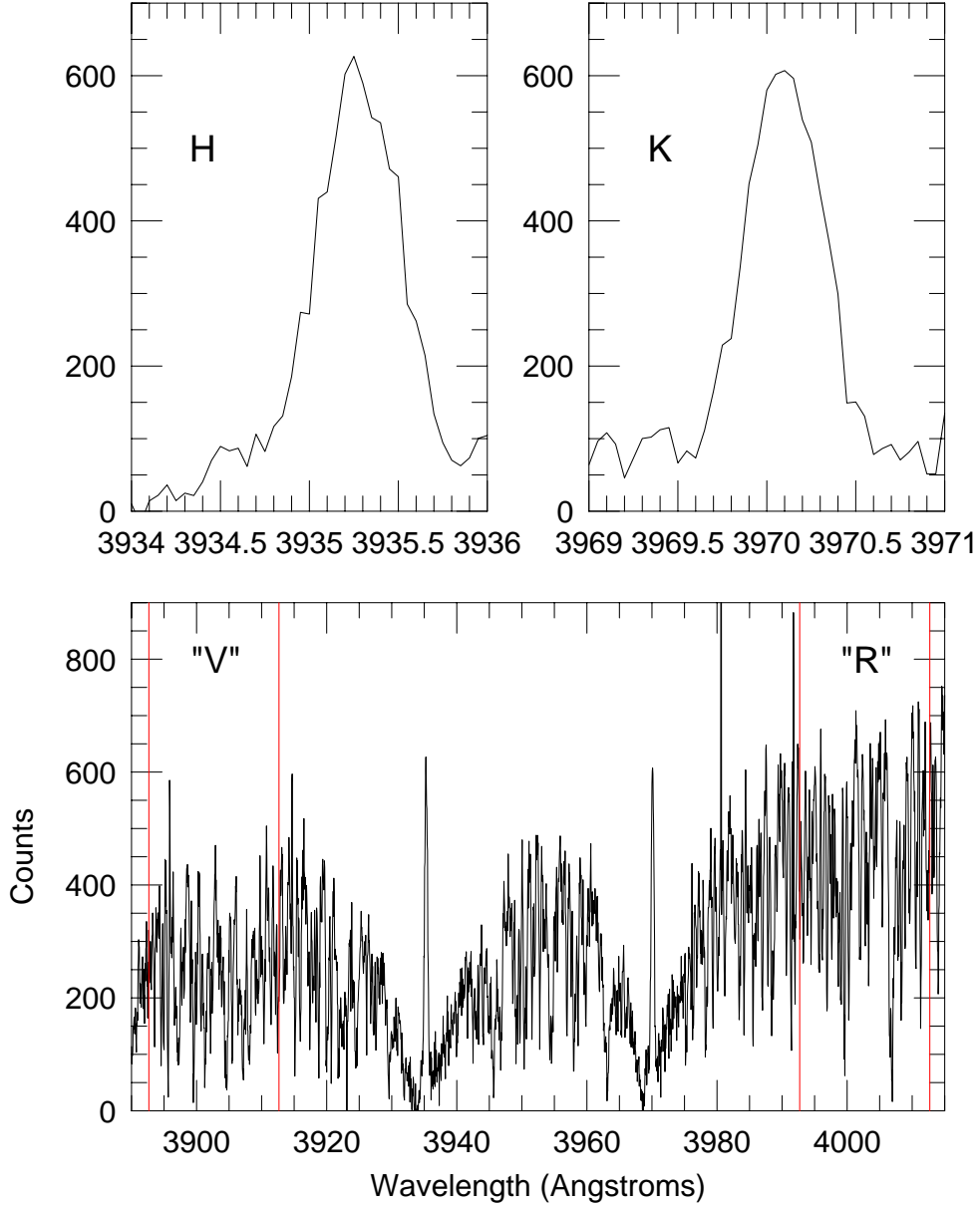


Fig. 3.— Lower panel: Bensby et al. (2011) UVES spectrum of MOA-2010-BLG-523S in the region of the calcium H & K lines. The mean counts per 0.05 \AA in V and R “continuum” passbands are 246 and 439, respectively. Upper Panels: Zooms of the cores of the calcium H & K lines. These have total counts of 5596 and 5297 respectively. Hence the S parameter is $S = (5596 + 5297)/[(246 + 439)/0.05 \text{ \AA}]$ or $S = 0.79 \text{ \AA}$.

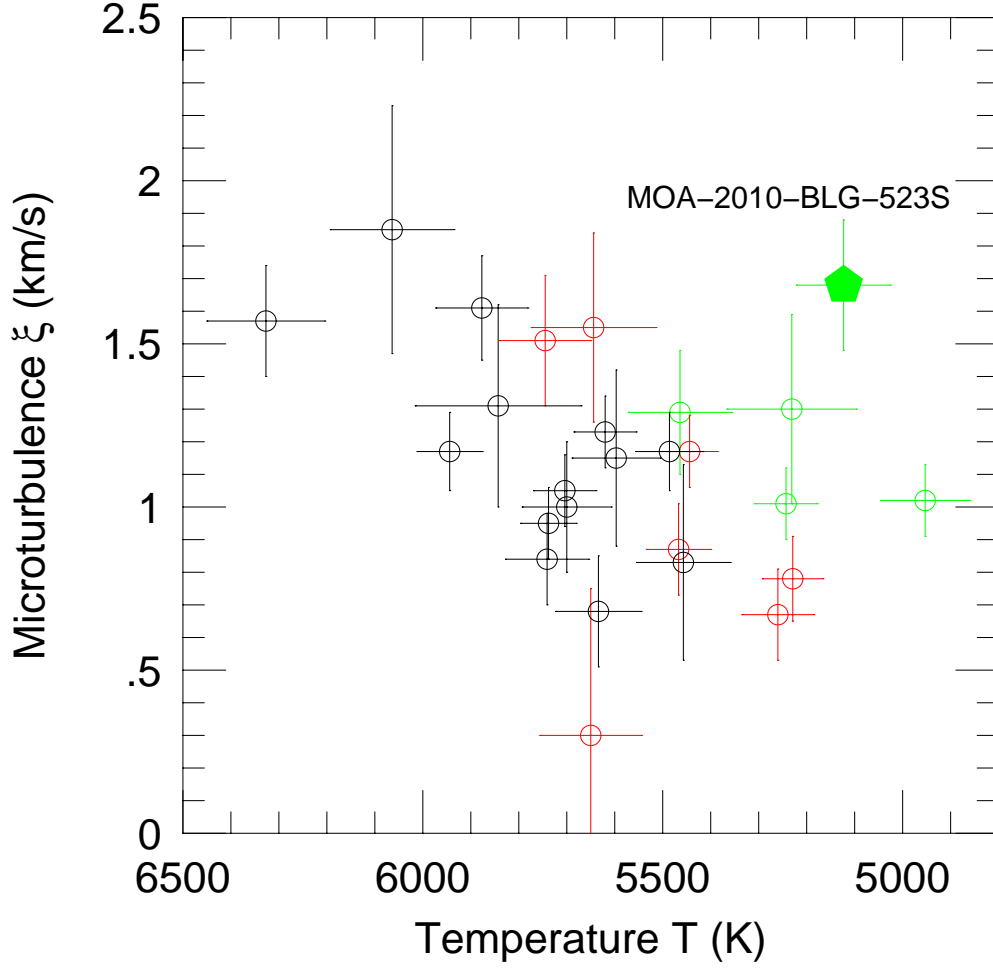


Fig. 4.— Microturbulence parameter ξ vs. temperature T for 26 microlensed dwarfs and subgiants measured by Bensby et al. (2010, 2011). “Dwarfs” ($\log g > 4.2$), “regular subgiants” ($4.0 \leq \log g < 4.2$), and “large subgiants” ($\log g \leq 4.0$) are shown in black, red, and green respectively. MOA-2010-BLG-523S is a clear outlier to the sample.

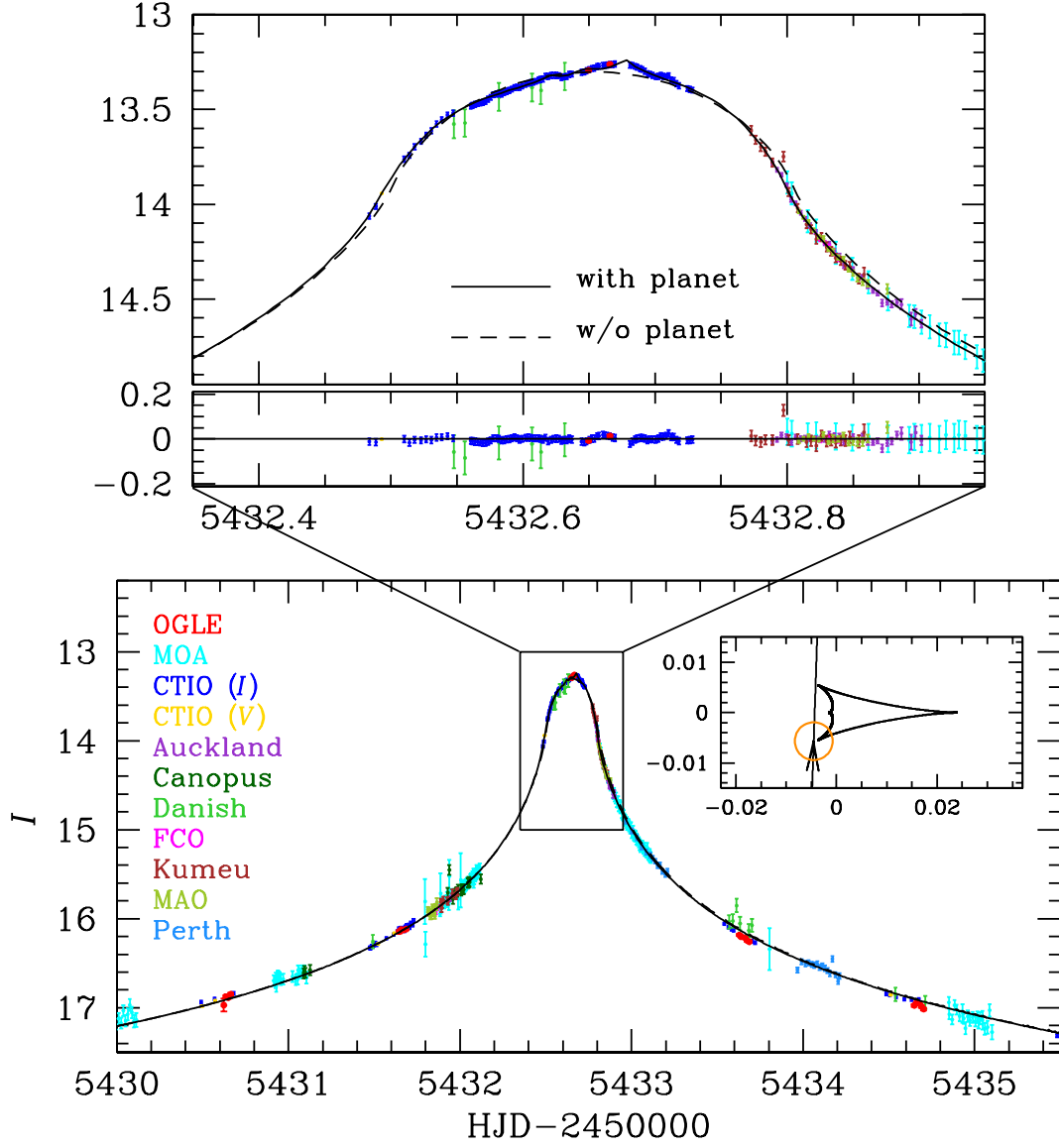


Fig. 5.— Planetary model of MOA-2010-BLG-523 (black) fit to I -band data points from several observatories as indicated in legend. H -band data are not shown.

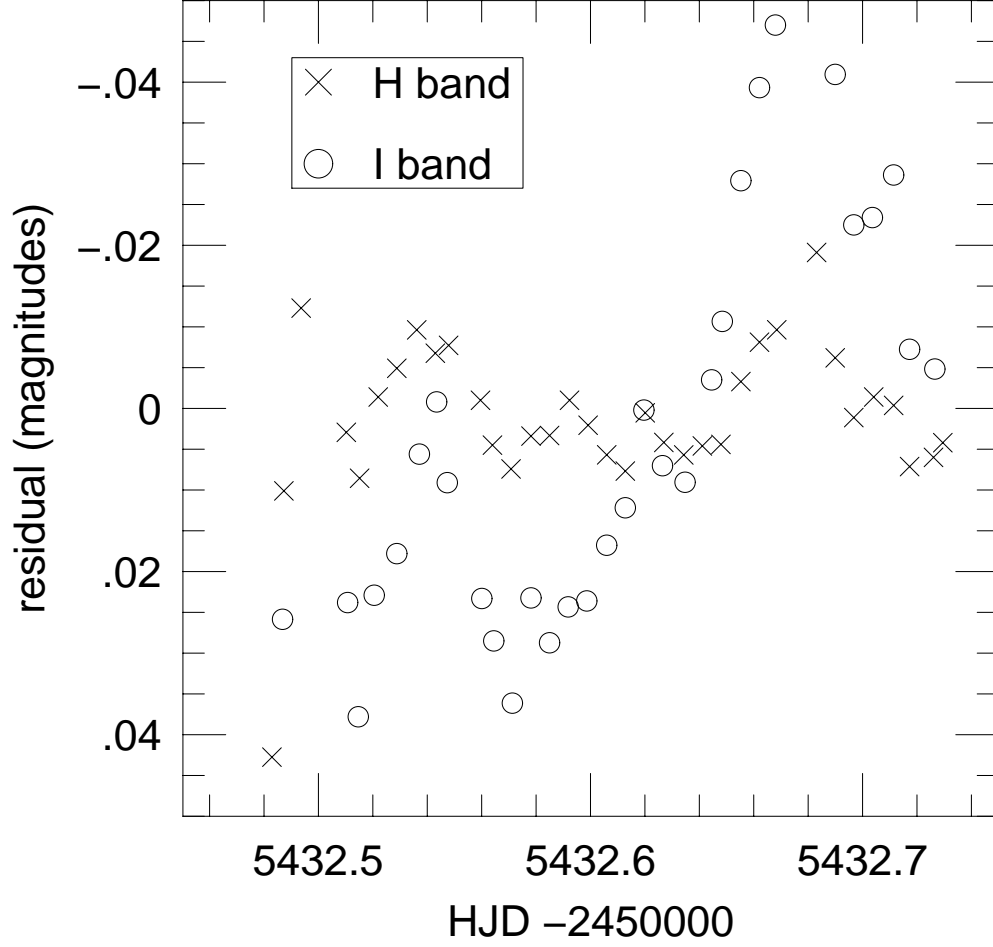


Fig. 6.— Residuals to a point-lens (finite source) fit that uses only *H*-band data over the peak, for CTIO *H*-band (crosses) and *I*-band (circles). Points are binned in 10-minute intervals. Error bars (not shown) are slightly smaller than points. In contrast to the *I*-band data, the *H*-band data show no convincing case for strong deviations.